IV.2 Celestial System Section of the Central Bureau

Introduction

The IAU charged the IERS with the responsibility of monitoring the International Celestial Reference System (ICRS) and maintaining its current realization, the International Celestial Reference Frame (ICRF), and links with other celestial reference frames. Starting in 2001, these activities are run jointly by the ICRS Product Center (Observatoire de Paris and US Naval Observatory) of the IERS and the International VLBI Service for Geodesy and Astrometry (IVS), in coordination with the IAU Working Group on the International Celestial Reference System. The present report was prepared by the Paris Observatory component of the ICRS Product Center, in cooperation with the ICRF section of the IERS Central Bureau that was in charge until the end of 2000.

The International Celestial Reference System (ICRS) is materialized by coordinates of extragalactic radio sources derived from VLBI observations. The access to ICRS in radio wavelengths is given by the 667 extragalactic radio sources in ICRF-Ext.1 (IERS, 1999). This extension of the initial ICRF was elaborated as a part of the maintenance process of the conventional celestial system and its frame (Ma *et al.*, 1997, 1998). While the set of the 212 defining sources and their respective coordinates remain unchanged with respect to the first realization of the frame, more precise coordinates for sources classified as “candidate” and “other” in ICRF are provided in ICRF-Ext.1; 59 “new” sources that were not included in the initial ICRF increase the number of objects in the conventional frame.

Concerning the ICRS monitoring, the location of the ICRS origin of right ascensions relative to the dynamical equinox is monitored using Lunar Laser Ranging (LLR) solutions. The location of the ICRS pole relative to the Celestial Ephemeris Pole is monitored using VLBI-derived celestial frames and time series of the celestial pole offsets.

Various investigations concerning ICRF-Ext.1 are presented, based on the contributions from VLBI analysis centers: additional sources since the construction of ICRF-Ext.1, stability analyses based on time series of source coordinates, and comparisons of the ICRF with newly computed radio source catalogues. Notice that some of these catalogues were generated from the TRF/EOP solutions rather than specifically for the CRF.

The ICRS Product Center at Paris Observatory organizes and updates a database which contains VLBI celestial frame realizations achieved during the last 15 years. Different files provide information to characterize the objects involved (radio source nomenclature, physical characteristics of radio sources, astrometric behaviour of a set of sources, radio source structure). The database is available at URL <http://hpiers.obspm.fr/icrs-pc>, by anonymous ftp (<hpiers.obspm.fr/icrs-pc>), and on request to the ICRS Product Center (<icrs-pc@hpopa.obspm.fr>).

The International Celestial Reference System

The kinematical definition of ICRS

Since 1998 January 1st, the International Celestial Reference Frame (ICRF), materialized by a set of extragalactic directions, replaced the Fifth Fundamental Catalogue (FK5) that gave star coordinates in a reference system (referred to as equator and equinox J2000.0) based primarily on the dynamics of the solar system (see Feissel and Mignard, 1998). The current definition of this conventional celestial reference system is based on a kinematical concept. In this concept, the axes of the system will remain fixed with respect to distant matter in the Universe. For the sake of continuity, the FK5 conventional directions at J2000.0 were retained in the new definition.

Figure IV-2.1 shows the positions of the mean pole and equinox at J2000.0 ($P_{J2000.0}$, $\gamma_{J2000.0}$) and those of the pole and the right ascensions origin of the FK5 catalogue (P_{FK5}, o_{FK5}) with respect to the ICRS pole and right ascensions origin (P_{ICRS}, o_{ICRS}).

Fig. IV-2.1: The ICRS pole and right ascensions origin.

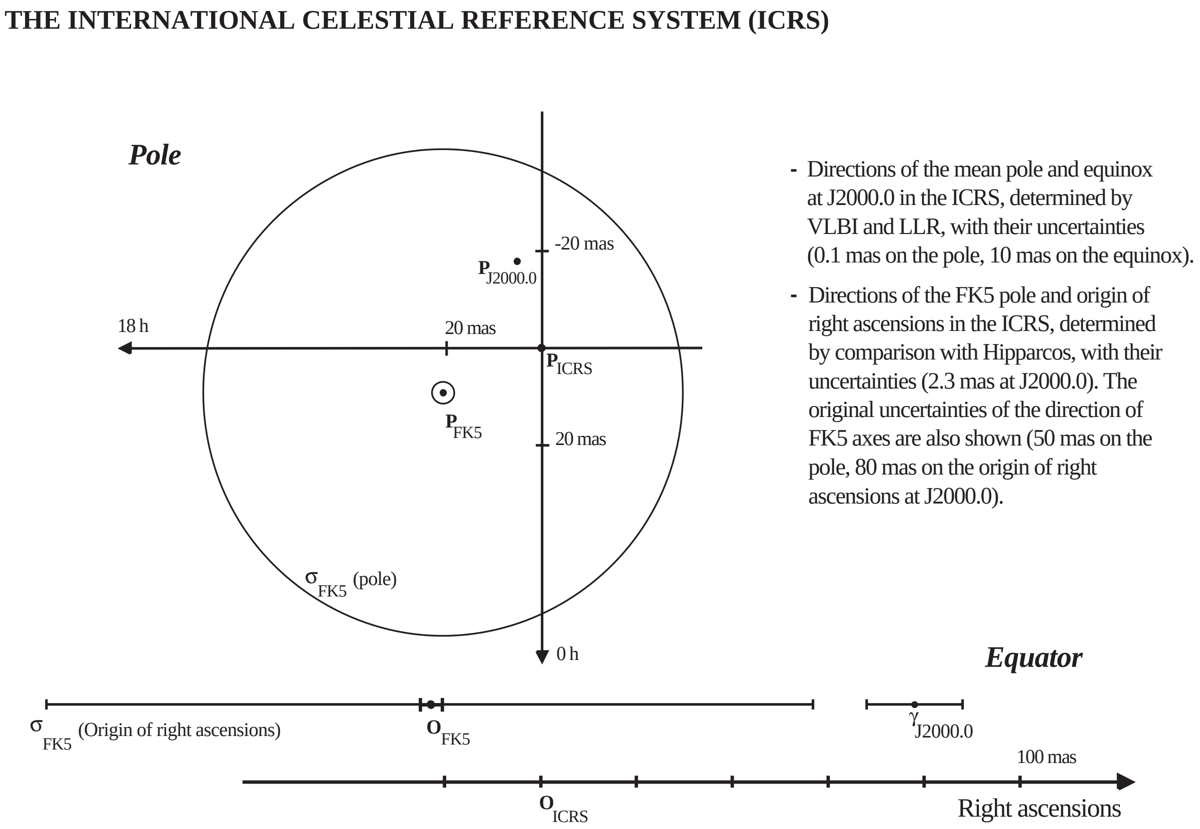

The origin of the coordinate axes in the ICRS is at the barycenter of the Solar System. The principal plane of the ICRS is close to the mean equator at J2000.0; it was defined by the equatorial plane implied in the IAU(1976) and IAU(1980) conventional precession and nutation models (Lieske *et al*., 1977; Seidelmann, 1982). In consistency with the IAU recommendations, the ICRS celestial pole agrees with that of the FK5 within the uncertainty of the latter (Fig. IV-2.1).

The right ascensions origin of the ICRS represents very closely the dynamical equinox at J2000.0, and agrees with the FK5 origin. It was implicitly defined in its first realization by adopting the mean of the J2000.0 right ascensions of 23 radio sources in a group of VLBI catalogues. These catalogues were compiled by fixing the right ascension of the quasar 1226+023 (3C273B) to its conventional FK5 value (obtained by Kaplan *et al*., 1982 from the FK4 value derived by Hazard *et al.,* 1971), a usual procedure at that time.

Ecliptic directions in ICRS

The combined analysis of VLBI and LLR observations (Folkner *et al.,* 1994) is one of the most efficient ways to determine the position of the planetary frame relative to the extragalactic reference frame. The series of Earth Orientation Parameters (EOP) adjusted in the analysis of VLBI observations provide the accurate relationship between the terrestrial reference system and the extragalactic celestial reference system. The LLR technique is sensitive to the orientation of the Earth with respect to the lunar orbit, providing fundamental information about the tie between the Earth-fixed frame and the dynamical frame materialized by the motion of the Moon as determined from semi-analytical theories or numerical integrations.

Thus knowing the station locations and the time-dependent rotation transformations involving the EOP, it is possible to infer the position of the planetary ephemeris frame with respect to the extragalactic reference frame. The orientation of the dynamical ecliptic and the location of the dynamical equinox in the ICRS are obtained from the combined analysis of the two techniques.

The definition of the ecliptic itself has been a subject of discussion (Standish, 1981; Kinoshita and Aoki, 1983). Following Le Verrier's definition, the ecliptic is the mean orbital plane of the Earth as determined from the secular part of the motion of the ascending node and the declination of the Sun with respect to an inertial reference plane.

The ecliptic can also be defined so that in the expression of the Sun's latitude there is no term containing the sine or the cosine of the argument of the latitude. Moreover, Standish (1981) pointed out that there can be two different definitions of the dynamical equinox and of the mean obliquity according to the way they are computed, that is, with respect to an inertial frame or to a rotating frame. The definition in a rotating frame is equivalent to Newcomb's one.

Monitoring the ICRS

Orientation of the celestial dynamical ecliptic reference frame from LLR results

In practice, the position of the inertial dynamical ecliptic at a given epoch with respect to the ICRS can be obtained from LLR observations. It must be emphasized that the lunar ephemerides (as ELP2000, DE405 etc...) provide the position of the inertial dynamical ecliptic with respect to the Moon, whereas the position of the equator of J2000.0 is implicitly given by its orientation with respect to the instantaneous equator at a given date by means of the nutation-precession matrix. In order to get the position of the dynamical ecliptic above, the complementary necessary parameters are the coordinates of the Celestial Ephemeris Pole (CEP), the Greenwich Sidereal Time (GST), the geocentric coordinates of the LLR stations (Folkner *et al.*, 1994) and the selenocentric coordinates of the receivers on the Moon. These last parameters can be subject to adjustment during the analysis.

The basic definitions concerned here are:

· the inertial dynamical ecliptic of J2000.0

· the J2000.0 mean equator (E) and origin of right ascensions (o)

· the inertial mean equinox of J2000.0 (γ_I) defined as the ascending node of the inertial ecliptic on the mean equator of J2000.0

The J2000.0 mean equator (E) and origin of right ascensions (o) are defined starting from both the rectangular coordinates of the LLR stations in the terrestrial reference frame and the adopted transformation from terrestrial coordinates to the celestial J2000.0 equatorial coordinates, with two realizations, according to the solutions OPA 01 M 01 and OPA 01 M 02 which are explained below (Fig. IV-2.2). The method is described in Chapront *et al.* (1999a).

Fig. IV-2.2: Position angles of the inertial mean ecliptic of J2000.0 according to the solutions OPA 01 M 01 and OPA 01 M 02

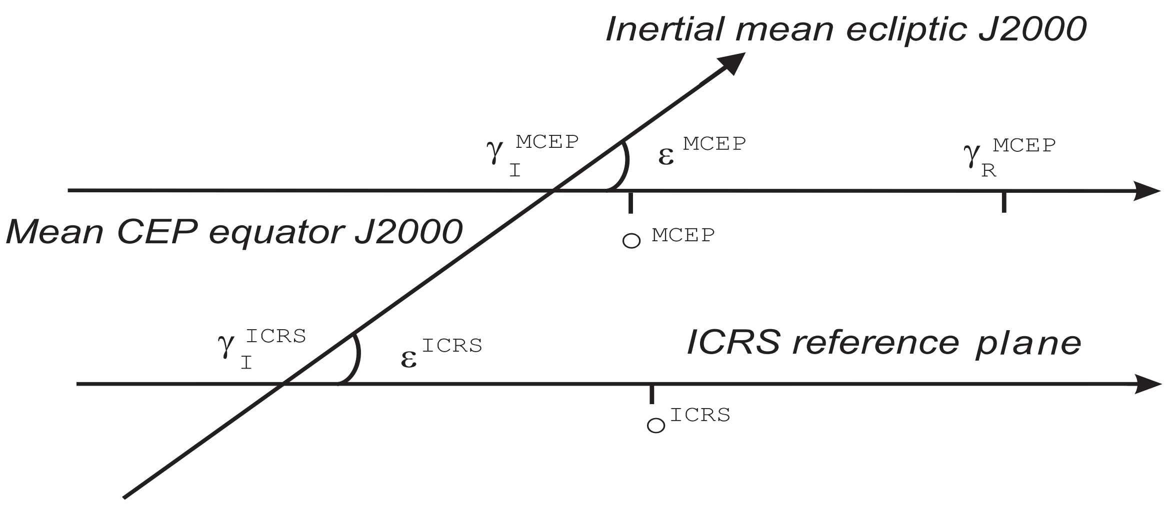

Solution OPA 01 M 01 gives the position of the inertial mean ecliptic of J2000.0 with respect to a celestial reference frame tied to the mean CEP equator of J2000.0. Solution OPA 01 M 02 gives the position of the inertial mean ecliptic of J2000.0 with respect to the ICRS.

These solutions result from weighted fits of the semi-analytical theory ELP 2000-96 of the orbital motion of the Moon (Chapront and Chapront-Touzé, 1997) and the improved Moon's analytical theory for the libration with numerical complements (Chapront *et al.*, 1999b). The numerical complements have been recently updated (Chapront, 2000).

These determinations are based on weighted fits of a lunar analytical solution to a set of 14 754 LLR observations (normal points) from McDonald (2.7 m telescope, MLRS1, MLRS2), Haleakala (Hawaii), and Grasse (CERGA), covering the time span from January 1972 till March 2001. A correction of 0.7 *ns* has been added to CERGA observations from 1997, January 13th till 1998, June 24th, in order to take into account a calibration offset mentioned by F. Mignard and J.-F. Mangin (CERGA). The adopted coordinates of McDonald 2.7 m, MLRS1, Haleakala transmitter and Grasse are those of ITRF94. The separations between MLRS2 and MLRS1, and Haleakala receiver and transmitter are constrained to JPL 1991 values. The velocities (plate motion) are given by ITRF94. The other corrections to the station coordinates are computed according to the IERS Standards (McCarthy, 1992). EOP values x, y, and UT1 are given by the IERS series EOP(IERS) C 04 and the short period variations are taken into account using Ray's developments in the IERS Conventions (McCarthy, 1996).

We present hereafter the two solutions: OPA 01 M 01 and OPA 01 M 02. The errors mentioned in these solutions represent the formal uncertainties resulting from the least squares adjustment. Realistic uncertainties can be estimated between five and ten times these values.

Analysis of the LLR solution OPA 01 M 01

In this solution, the precession is given by the expressions of Williams (1994) with corrections to the precession and obliquity constants introduced by means of the derivatives of Simon *et al.* (1994). The nutation adopted is from Herring (McCarthy, 1996). The conclusions by Williams and Melbourne (1982) are taken into account by means of a correction to the sidereal time. The resulting J2000.0 celestial equator and origin of right ascensions are denoted as J2000.0 mean CEP equator and CEP origin of right ascensions. The notation for this origin is o^{MCEP}.

The solution yields the fitted values of the inertial mean obliquity of J2000.0 ε_I^{MCEP}, the arc $o^{MCEP}\gamma_I^{MCEP}$ along the equator, and the correction Δp to the IAU 1976 precession constant:

$$\varepsilon_I^{MCEP} = 23° \, 26' \, 21''.405\,62 \pm 0.000\,05''$$

$$o^{MCEP}\gamma_I^{MCEP} = -14.5 \pm 0.2 \; mas$$

$$\Delta p = -3.36 \pm 0.03 \; mas/yr$$

Usually, γ_I^{MCEP} is named the «inertial dynamical mean equinox» of J2000.0. The separation from γ_I^{MCEP} to the «rotational dynamical mean equinox» of J2000.0 γ_R^{MCEP} is 93.66 *mas* (Standish, 1981). γ_R^{MCEP} is the same as $\gamma_{J2000.0}$ in Fig. IV-2.1.

Analysis of the LLR solution OPA 01 M 02

In this solution, the precession-nutation resulted from the corrections $d\psi$ and $d\varepsilon$ given by the series EOP(IERS) C 04. The resulting J2000.0 celestial equator and origin of right ascensions stand for the ICRS equator and origin of right ascensions. The latter origin is denoted as o^{ICRS}.

The solution yields the fitted values of the mean obliquity ε_I^{ICRS} and the arc $o^{ICRS}\,\gamma_I^{ICRS}$ along the equator:

$$\varepsilon_I^{ICRS} = 23° \, 26' \, 21''.411\,08 \pm 0.000\,05''$$

$$o^{ICRS}\,\gamma_I^{ICRS} = -55.3 \pm 0.1 \; mas$$

The difference between the two lunar mean longitudes at the weighted mean epoch of observations gives the arc $\gamma_I^{ICRS}\,\gamma_I^{MCEP}$ separating the two inertial equinoxes in the dynamical ecliptic of J2000.0:

$$\gamma_I^{ICRS}\,\gamma_I^{MCEP} = 44.5 \pm 0.4 \; mas$$

Orbital parameters of the Moon and of the Earth-Moon barycenter, free libration parameters, tidal secular acceleration, corrections to the theoretical values of the mean motions of the lunar perigee and of the node have also been fitted in both solutions (Chapront *et al.*, 2001).

Direction of the mean pole at J2000.0 in the ICRS from VLBI results

Until 2000, the IERS Conventions (McCarthy, 1996) provided a rate correction to the IAU (1976) precession in longitude and a rate in obliquity which was ignored in the current IAU models as well as a state of the art nutation model that was implicitly referred to the mean pole at J2000.0. In 2000, the IAU recommended the use of a new nutation model, MHB2000 (Mathews *et al.*, 2001), starting from 2003, January 1st. On the other hand, the ICRS pole was defined in 1988 by using the then current IAU models (Lieske *et al.,* 1977; Seidelmann, 1982). To the extent that the IERS(1996) nutation model or the MHB2000 are accurate, VLBI time series of the celestial pole offsets $d\psi$, $d\varepsilon$, referred to the ICRF pole, can be used to estimate the direction of the mean pole at J2000.0 in the ICRS ($P_{J2000.0}$ in Fig. IV-2.1).

The IERS series of $d\psi$, $d\varepsilon$ (e.g. EOP(IERS) C 04) are referred to the ICRS. If we correct them by the IERS(1996) precession-nutation model, or if we use the MHB2000 model and the corresponding precession and obliquity rates corrections (resp. –2.997 mas/year and –0.255 mas/year), the expected remaining signal, apart from the Free Core Nutation, is a pair of biases $d\psi_0$, $d\varepsilon_0$ that reflect the misalignment of the mean pole at J2000.0 with the ICRS pole. Defining the rotation around the ICRS X-axis as P_18h and the rotation around the ICRS Y-axis as P_0h, one gets:

$$P\_18h = -\,d\varepsilon_0; \qquad P\_0h = d\psi_0 \sin \varepsilon_0$$

In the case of a VLBI solution that includes both a series of $d\psi$, $d\varepsilon$ and a celestial reference frame (CRF), the same information can be derived after taking into account the corrections that bring the results into the IERS system. Using the VLBI solutions submitted for this Annual Report, the angles between individual CRF and the ICRF and the consistency corrections, estimations of P_18h and P_0h, are given in Table IV-2.1.a, using the IERS(1996) precession-nutation model, and in Table IV-2.1.b, using the MHB2000 model.

Table IV-2.1.a: Coordinates of the mean pole at J2000.0 in the ICRS, based on individual solutions and on the IERS results, using the nutation series EOP(IERS) C 04, corrected by the IERS(1996) precession-nutation model

EOP		RSC		Time span	P_0h	P_18h
BKGI	01 R 01	BKGI	01 R 01	1984.0-2001.0	-17.15±0.02	5.10±0.02
GSFC	01 R 01	GSFC	01 R 01	1979.0-2001.0	-17.12±0.01	5.09±0.01
IAA	01 R 01	IAA	01 R 02	1984.0-2001.0	-17.15±0.03	5.06±0.03
SHA	01 R 01	SHA	01 R 01	1979.0-2001.0	-17.13±0.03	5.10±0.03
IERS	C 04	ICRF-Ext.1		1984.0-2001.0	-16.94±0.08	5.07±0.01

Unit: 0.001"

Table IV-2.1.b: Coordinates of the mean pole at J2000.0 in the ICRS, based on individual solutions and on the IERS results, using the nutation series MHB2000

EOP		RSC		Time span	P_0h	P_18h
BKGI	01 R 01	BKGI	01 R 01	1984.0-2001.0	-16.63±0.02	6.80±0.02
GSFC	01 R 01	GSFC	01 R 01	1979.0-2001.0	-16.60±0.01	6.76±0.01
IAA	01 R 01	IAA	01 R 02	1984.0-2001.0	-16.59±0.03	6.81±0.03
SHA	01 R 01	SHA	01 R 01	1979.0-2001.0	-16.61±0.03	6.77±0.03
IERS	C 04	ICRF-Ext.1			-16.41±0.02	6.80±0.02

Unit: 0.001"

In order to evaluate the position of the mean pole at J2000.0 with respect to the ICRF, we calculated the mean value of the coordinates P_18h and P_0h given by the tables above. We conclude that the direction of the mean pole at J2000.0 in the ICRS is 5.0 *mas* in the direction 18h and 17.1 *mas* in the direction 12h, when we adopt as a nutation model the IERS(1996) one, and respectively 6.8 *mas* and 16.6 *mas*, when we adopt the MHB2000 nutation model. Note that the difference of determinations between the two models are not detectable at the scale of Fig. IV-2.1. As a consequence, in order to predict $d\psi$ and $d\varepsilon$ in the ICRS by means of the IERS(1996) precession-nutation model or by means of the MHB2000 model, one must use a pair of additive constants, which are:

– in longitude : $d\psi_0 = -0.0431''$ [IERS(1996)];
$d\psi_0 = -0.0417''$ (MHB2000).
– in obliquity : $d\varepsilon_0 = -0.0051''$ [IERS(1996)];
$d\varepsilon_0 = -0.0068''$ (MHB2000).

These constants will be absorbed in the expressions for precession/nutation to be used after 2003, January 1st.

Investigations concerning ICRF-Ext.1

Additional sources

In the frames submitted this year to IERS, 21 extragalactic radio sources not present in ICRF-Ext.1 are found. Most of these sources have a short observational history and in consequence only preliminary ICRS coordinates can be obtained from the individual catalogues by using the parameters of Tables IV-2.-6 and IV-2.7 to transform individual frames into ICRS. The Table IV-2.2 gives ICRF designations and the source information available in each frames.

Table IV-2.2: Additional sources with respect to ICRF-Ext.1

ICRF Designation	IERS Des.	Frame	Mean MJD	First of observation	Last span	Nb ses.	Nb Delay
J024031.6+611345	0236+610						
		RSC(BKGI) 01 R 01	50492.2	49693.8	51736.8	22	62
		RSC(GSFC) 01 R 01	50262.4	49690.0	51975.7	28	87
		RSC(IAA) 01 R 02	50798.5	49980.1	51674.7	13	40
		RSC(SHA) 01 R 01	50493.2	49694.8	51961.8	26	62
J032536.8+222400	0322+222						
		RSC(BKGI) 01 R 01	51614.6	51323.8	51813.8	16	170
		RSC(GSFC) 01 R 01	51492.9	51324.8	51814.8	19	742
		RSC(IAA) 01 R 02	51563.0	51323.8	51814.4	14	184
		RSC(SHA) 01 R 01	51470.5	51324.8	51814.8	17	491
J032754.1+023341	0325+023						
		RSC(IAA) 01 R 02	51492.3	51492.1	51492.4	1	4
		RSC(SHA) 01 R 01	51492.8	51492.8	51787.8	2	4

J033647.3+003519	0334+004								
		RSC(IAA)	01 R 02	49987.3	49987.3	49987.4	1	2
		RSC(SHA)	01 R 01	49992.8	49987.8	50064.8	3	3
J041821.2+380135	0415+379							
		RSC(GSFC)	01 R 01	51534.1	51464.8	51681.7	5	135
		RSC(IAA)	01 R 02	51538.2	51464.1	51681.7	4	46
		RSC(SHA)	01 R 01	51538.3	51464.8	51681.7	4	47
J065917.9+081330	0656+082							
		RSC(IAA)	01 R 02	51584.9	51520.2	51688.6	4	39
		RSC(SHA)	01 R 01	51583.6	51520.8	51688.8	4	38
J094014.7+260329	0937+262							
		RSC(BKGI)	01 R 01	51407.8	51407.8	51407.8	1	13
		RSC(IAA)	01 R 02	51408.0	51407.8	51408.6	1	13
		RSC(SHA)	01 R 01	51408.8	51408.8	51408.8	1	13
J094538.1+353455	0942+358							
		RSC(GSFC)	01 R 01	50854.6	50854.6	50854.6	1	100
J124129.5+602041	1239+606							
		RSC(IAA)	01 R 02	51367.9	51352.0	51352.7	2	9
		RSC(SHA)	01 R 01	51368.3	51352.8	51380.7	2	9
J141604.1+344436	1413+349							
		RSC(GSFC)	01 R 01	51684.3	51646.8	51687.6	2	63
		RSC(IAA)	01 R 02	51646.3	51645.8	51646.7	1	4
		RSC(SHA)	01 R 01	51646.8	51646.8	51646.8	1	4
J143853.6+371035	1436+373							
		RSC(GSFC)	01 R 01	51687.6	51687.6	51687.6	1	65
J143923.6+325354	1437+331							
		RSC(GSFC)	01 R 01	51687.6	51687.6	51687.6	1	35
J181657.0+530744	1815+531							
		RSC(BKGI)	01 R 01	51703.5	51703.5	51703.5	1	11
		RSC(SHA)	01 R 01	51704.5	51704.5	51704.5	1	11
J192218.6+084157	1919+086							
		RSC(SHA)	01 R 01	50700.6	50700.6	50700.6	1	9
J192439.4+154043	1922+155							
		RSC(GSFC)	01 R 01	50654.8	50654.8	50654.8	1	339
J200210.4+472528	2000+472							
		RSC(BKGI)	01 R 01	51703.5	51703.5	51703.5	1	27
		RSC(GSFC)	01 R 01	51704.5	51704.5	51704.5	1	27
		RSC(SHA)	01 R 01	51704.5	51704.5	51704.5	1	27
J210841.0+143027	2106+143							
		RSC(GSFC)	01 R 01	50800.8	50800.8	50800.8	1	296
J212313.3+100754	2120+099							
		RSC(BKGI)	01 R 01	50699.6	50699.6	50699.6	1	38
		RSC(GSFC)	01 R 01	50700.6	50700.6	50700.6	1	31
		RSC(SHA)	01 R 01	50700.6	50700.6	50700.6	1	56
J214518.7+111527	2142+110							
		RSC(GSFC)	01 R 01	50654.8	50654.8	50654.8	1	124
J214755.2+083011	2145+082							
		RSC(GSFC)	01 R 01	50654.8	50654.8	50654.8	1	26
J214935.2+075625	2147+077							
		RSC(BKGI)	01 R 01	50699.6	50699.6	50699.6	1	24
		RSC(SHA)	01 R 01	50700.6	50700.6	50700.6	1	30

Source stability analyses

The astrometry data set used here is a time series of session-per-session source positions computed in a homogeneous reference frame by T. M. Eubanks, then at USNO, from VLBI observations going back to August 1979. For the most regularly observed sources, quasi continuous time series of weighted average coordinates at one-year intervals are shown on the ICRS-PC website: <http://hpiers.obspm.fr/icrs-pc/timeseries/presentation.html>.

Figure IV-2.3 shows source stability plots under the form of the envelopes of the standard deviation of 0.5 year averages in the source declinations and right ascensions. The figure presents separately the sources with high or moderate stability and those with low stability, measured over 1987–1999.

Table IV-2.3 gives the distribution of the maximum variance directions as a function of declinations for the two classes of sources shown in Fig. IV-2.3.

Table IV-2.4 gives the amplitude and direction of the maximum standard deviations over 1994–1999 for 258 sources with a good observational history over that time span.

The most stable sources show a quite even distribution of the local directions of maximum variability in the declination zones north of +20° and south of –20°, suggesting that the observed variability corresponds to real local effects in the sources. A detailed study of the 16 best observed sources north of declination +20° (Feissel *et al.*, 2000) shows that the VLBI results are precise enough to allow the spectral characterization of the source variability. However, the results in the declination zone [–20°,+20°] show an excess of the variability in the direction of declinations, probably reflecting tropospheric mismodelling. This excess is much stronger for the more variable sources, for which an even distribution is reached only north of +20°. An extensive analysis of the time stability of nearly 300 ICRF sources is being published (Gontier et *al.*, 2001).

Table IV-2.3: Distribution of the angles of axes of maximum variability with respect to the declination axis, for sources shown on Fig. IV-2.3.

Declinations in degrees	Inclination bins (absolute values) Stable sources			Unstable sources		
	0°-30°	30°-60°	60°-90°	0°-30°	30°-60°	60°-90°
+20 to +90	35%	42%	23%	32%	45%	23%
0 to +20	55%	27%	18%	55%	31%	14%
-20 to 0	55%	30%	15%	67%	20%	13%
-90 to -20	42%	26%	32%	70%	18%	12%

Fig. IV-2.3: Envelopes of the 1987–1999 standard deviations of 0.5 year averages in equatorial coordinates. Sources with a) high or moderate stability, b) with low stability.

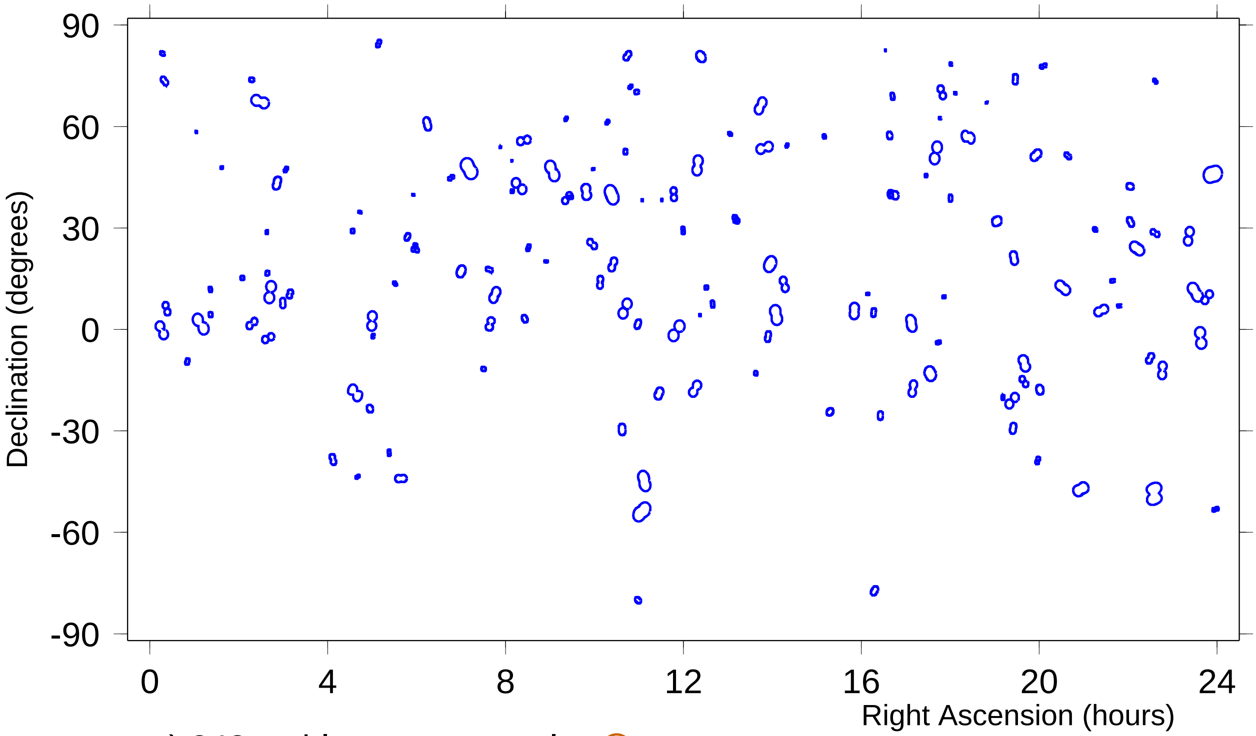

a) 243 stable sources, scale: ◯ (Diameter = 0,001")

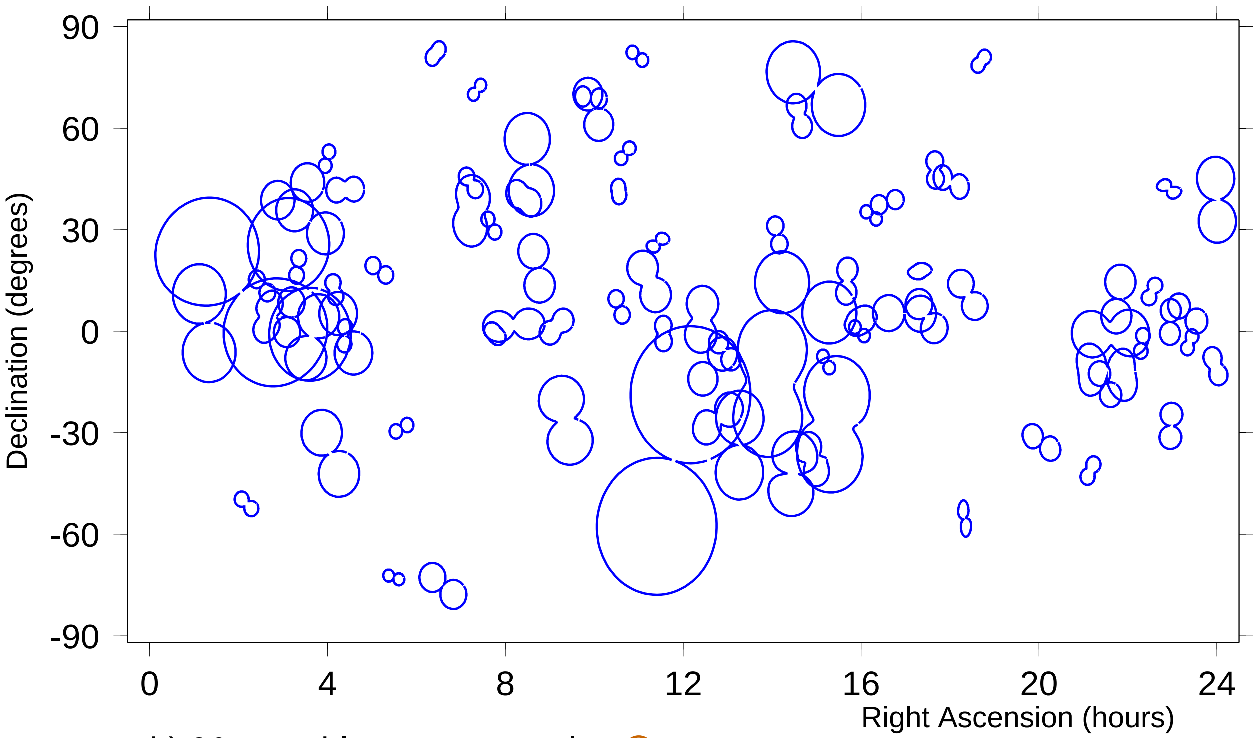

b) 86 unstable sources, scale: ◯ (Diameter = 0,001")

Table IV-2.4:
Stability criteria of ICRS sources

Struc: The ICRF-Ext.1 structure indices in the S and X bands (1->4, in decreasing order of astrometric suitability).
Sigmax: Standard error of average residuals at 0.5 year intervals, in direction Dir.
Dir: Direction of the maximum variance relative to the local parallel (90° ~ declinations axis, 0 & 180° ~ right ascensions axis).
Data span: Dates of the first and last average points considered (years-1900).
Np: Number of average points at 0.5 year intervals available in the data span.
Ns: Number of sessions having the source over 1980.00-1999.25.

Source	Struc S X	Sigmax (mas)	Dir (deg)	Data span	Np	Ns
0003-066	3 1	.169	92.	94.5-99.0	8	200
0013-005	2 1	.467	110.	96.0-99.0	7	30
0014+813	1 1	.080	58.	94.0-99.0	11	269
0016+731	2 1	.302	136.	94.0-98.5	9	401
0019+058	1 1	.341	106.	95.0-98.0	5	13
0048-097	1 1	.117	84.	94.0-99.0	11	709
0055+300		.961	92.	96.5-99.0	5	8
0059+581	2 1	.052	122.	94.0-99.0	11	622
0104-408		.225	110.	94.0-99.0	11	265
0106+013	2 1	.501	114.	94.0-99.0	11	1017
0111+021	3 1	.180	46.	94.5-99.0	10	94
0119+041	2 1	.101	106.	94.0-99.0	11	1208
0119+115	2 1	.134	104.	95.5-99.0	8	141
0133+476	2 1	.050	24.	94.0-99.0	10	286
0146+056	3 1	.585	30.	96.0-99.0	7	30
0201+113	2 1	.175	102.	94.0-99.0	11	215
0202+149	2 2	.092	44.	94.0-99.0	11	338
0202+319	2 2	.200	64.	95.0-99.0	6	18
0202-172	3 1	.661	116.	94.5-98.0	5	11
0208-512		.819	138.	94.0-99.0	11	212
0212+735	2 2	.190	40.	94.0-99.0	8	1122
0215+015	1 1	.220	20.	94.0-98.5	8	18
0220-349		.684	54.	94.0-98.5	6	9
0221+067	2 2	.527	40.	95.5-98.0	6	9
0229+131	2 1	.088	148.	94.0-99.0	11	1578
0234+285	3 2	.081	110.	94.0-99.0	9	877
0235+164	1 1	.131	98.	94.0-99.0	11	212
0236+610		2.114	26.	95.0-99.0	5	9
0237+040	2 1	1.020	62.	94.5-98.5	5	11
0237-027	1 1	.330	16.	94.5-99.0	6	11
0238-084	4 2	.270	36.	94.5-99.0	10	165
0239+108	2 2	.568	78.	95.5-99.0	8	29
0256+075	2 1	.109	94.	95.5-98.0	5	31
0300+470	2 1	.173	88.	94.0-98.5	8	662
0302-623		.240	32.	94.0-96.5	5	14
0305+039		.268	20.	96.5-99.0	5	12
0306+102	3 1	.224	64.	96.0-98.5	6	22
0308-611		.191	118.	94.0-96.5	6	55
0317+188	2 1	.826	78.	96.0-98.5	6	22
0333+321	3 3	.112	174.	94.0-99.0	7	57
0336-019	2 1	.136	162.	94.0-99.0	11	512
0338-214		.699	108.	94.0-99.0	9	21
0341+158	2 1	.160	124.	95.0-97.5	5	9

Table IV-2.4 (cont.)

Source	Struc S	Struc X	Sigmax (mas)	Dir (deg)	Data span	Np	Ns
0355+508	2	3	.679	84.	94.0-98.0	5	358
0402-362			2.223	114.	94.0-99.0	11	154
0405-385			.249	112.	95.5-99.0	6	34
0420-014	3	1	.658	76.	94.0-99.0	9	1168
0422+004	2	1	.536	84.	95.0-98.5	5	12
0430+052	4	3	.788	98.	94.5-99.0	8	51
0430+289			.111	90.	96.0-99.0	7	26
0434-188	3	1	.643	124.	94.0-98.5	8	48
0437-454			.649	72.	94.0-98.0	6	10
0440+345	2	1	.099	166.	94.5-98.5	6	14
0440-003	1	1	.657	4.	94.5-98.0	5	15
0454+844	2	1	.178	64.	94.0-98.5	8	21
0454-234	2	1	.191	144.	94.0-99.0	11	1302
0457+024	4	1	.470	80.	94.0-99.0	10	43
0458-020	2	1	.102	58.	94.0-99.0	11	906
0507+179	2	2	.156	68.	94.5-98.5	5	23
0521-365			.335	110.	94.5-99.0	8	44
0528+134	1	1	.124	148.	94.0-99.0	11	2118
0528-250			.658	102.	94.0-98.5	6	14
0530-727			.322	150.	94.0-97.0	7	34
0537-441	3	1	.318	0.	94.0-98.5	10	268
0539-057	2	1	.396	52.	94.0-98.0	6	9
0544+273	1	1	.198	54.	95.0-98.5	7	21
0552+398	2	1	.043	166.	94.0-99.0	11	2488
0554+242			.201	30.	96.0-98.5	5	17
0556+238	1	1	.210	112.	95.5-99.0	8	112
0605-085	3	1	.390	0.	94.5-98.0	5	10
0607-157	2	2	.238	146.	94.0-97.0	5	8
0615+820	3	1	.397	150.	94.0-97.0	5	19
0620+389			.349	52.	94.0-97.0	5	8
0636+680	1	1	.344	158.	94.0-96.5	5	26
0637-752			.231	0.	94.0-99.0	11	222
0642+449	1	1	.056	38.	94.0-99.0	11	277
0648-165	2	1	.696	158.	94.5-97.0	5	7
0657+172	2	1	.270	74.	94.0-98.5	9	86
0716+714	1	1	.167	136.	94.0-98.0	6	79
0718+792	2	1	.114	142.	94.0-99.0	11	223
0723-008	3	2	.522	18.	94.0-98.5	6	19
0727-115	1	1	.112	148.	94.0-99.0	11	1666
0735+178	3	1	.129	164.	94.0-98.5	9	463
0736+017	3	3	.333	58.	95.5-99.0	8	23
0742+103	4	1	.462	82.	94.0-98.5	8	268
0743+259	1	1	.364	2.	94.5-98.0	5	7
0745+241	3	2	.179	52.	96.0-99.0	7	100
0749+540	1	1	.055	30.	94.0-99.0	11	152
0804+499	2	1	.042	118.	94.0-99.0	11	450
0805+410	2	1	.098	58.	94.0-99.0	11	115
0814+425	2	1	.152	0.	94.0-97.5	7	109
0818-128	3	1	1.562	94.	94.5-98.5	6	14
0820+560	2	1	.390	10.	94.0-99.0	6	48
0821+394	2	2	.224	166.	94.0-98.5	5	12
0821+621			.473	30.	94.0-99.0	6	8
0823+033	2	1	.151	114.	94.0-99.0	11	547
0826-373			1.258	106.	94.5-98.5	5	9
0827+243	2	2	.161	64.	94.5-98.5	5	30
0839+187	4	3	1.716	98.	94.0-98.5	7	16

Table IV-2.4 (cont.)

Source	Struc S X	Sigmax (mas)	Dir (deg)	Data span	Np	Ns
0851+202	2 1	.077	170.	94.0-99.0	11	2222
0906+015	3 2	.309	104.	94.5-98.0	5	14
0917+624	2 1	.107	54.	94.5-99.0	10	59
0919-260	3 2	1.272	74.	94.0-99.0	11	223
0920+390		.341	46.	95.0-99.0	9	34
0920-397		.870	90.	95.0-98.5	7	32
0923+392	2 1	.100	30.	94.0-99.0	11	2279
0951+693		.905	168.	94.0-99.0	11	42
0952+179	3 3	.269	76.	94.5-98.5	5	25
0953+254	2 1	.341	136.	94.0-99.0	11	388
0954+658	2 1	1.747	110.	94.0-99.0	11	236
0955+476	1 1	.069	30.	94.0-99.0	11	707
1004+141	3 2	.316	84.	94.0-99.0	11	161
1014+615		.141	42.	94.0-98.5	7	13
1022+194	2 2	.355	66.	95.0-98.5	6	12
1032-199		1.388	130.	95.0-98.5	5	8
1034-293	1 1	.238	92.	94.0-99.0	11	810
1038+064	3 1	.403	56.	95.0-98.5	7	31
1038+528		.137	76.	94.0-99.0	11	121
1039+811	2 1	.169	32.	94.0-97.5	5	12
1044+719	1 1	.124	36.	94.0-99.0	11	313
1053+704	1 1	.130	68.	94.0-99.0	8	23
1053+815	1 1	.690	144.	94.0-99.0	9	90
1055+018	2 2	.202	48.	94.5-98.5	6	205
1057-797		.158	134.	94.0-99.0	11	189
1101+384	1 1	.060	106.	94.5-99.0	10	90
1101-536		.539	42.	94.0-99.0	7	26
1104-445		.431	94.	94.0-98.0	8	160
1123+264	2 1	.225	82.	94.0-97.0	6	84
1124-186	1 1	.205	54.	94.5-99.0	10	214
1128+385	1 1	.061	82.	94.0-99.0	11	480
1130+009	2 1	.793	86.	94.0-98.5	7	14
1144+402	1 1	.269	94.	94.0-99.0	8	96
1144-379		.170	122.	94.5-99.0	10	212
1145-071	3 1	.194	36.	94.0-98.5	10	81
1156+295	2 2	.191	90.	94.0-99.0	11	376
1213-172	1 1	.434	52.	94.0-98.5	5	11
1219+044	2 1	.056	80.	94.0-99.0	11	554
1219+285	3 2	.135	158.	95.5-99.0	5	13
1221+809	2 1	.281	146.	94.0-98.5	7	14
1222+037	4 2	.262	4.	94.0-98.5	6	44
1222+131		.781	76.	96.5-99.0	5	10
1226+373	1 1	.554	50.	94.0-98.5	7	10
1228+126	3 3	.139	54.	95.0-99.0	9	220
1236+077	2 1	.169	86.	94.5-99.0	6	12
1237-101		1.641	46.	94.0-99.0	7	13
1243-072	2 1	.192	90.	94.5-98.5	7	23
1244-255		.130	128.	94.0-98.5	7	51
1253-055	3 2	1.500	142.	95.0-98.5	7	187
1255-316		1.350	106.	94.5-99.0	10	68
1300+580	1 1	.119	148.	94.0-99.0	11	91
1302-102	2 1	.973	120.	94.0-99.0	9	22
1308+326	1 1	.137	58.	94.0-99.0	11	1138
1308+328		.247	130.	95.0-99.0	8	23
1313-333	1 1	2.720	88.	94.5-99.0	10	86
1334-127	2 1	.083	66.	94.0-99.0	11	1323

Table IV-2.4 (cont.)

Source	Struc S X	Sigmax (mas)	Dir (deg)	Data span	Np	Ns
1349-439		2.731	56.	94.0-99.0	5	7
1351-018	1 1	.252	92.	94.0-99.0	11	213
1354+195	3 2	.167	158.	94.0-98.5	8	60
1354-152	1 1	.325	4.	95.0-99.0	5	67
1357+769	1 1	.037	104.	94.0-99.0	11	527
1402+044	2 1	.389	74.	94.0-99.0	9	36
1404+286	3 1	.431	102.	94.5-99.0	10	1024
1406-076	2 1	.113	26.	94.0-99.0	7	19
1413+135	1 3	.432	116.	95.5-99.0	7	16
1418+546	2 2	.071	54.	95.5-99.0	8	193
1424-418		.330	146.	94.0-99.0	11	191
1442+101	3 3	2.992	150.	94.0-98.0	5	27
1451-375		1.451	108.	95.0-99.0	7	50
1451-400		.786	64.	94.0-98.5	7	22
1458+718	3 3	.436	84.	94.0-98.0	6	13
1504-166	3 1	4.454	20.	95.0-99.0	7	22
1508+572		.101	130.	94.5-99.0	10	39
1510-089	3 1	.588	104.	94.0-99.0	9	250
1511-100	1 1	.706	110.	94.0-98.0	6	8
1514-241		.209	32.	94.5-99.0	9	93
1519-273		.481	52.	94.0-99.0	10	89
1546+027	2 1	.344	58.	95.5-98.5	5	16
1548+056	2 2	.166	64.	94.0-98.5	7	209
1555+001	1 1	.652	134.	95.0-99.0	7	80
1557+032		.937	18.	94.5-99.0	9	23
1600+335	3 1	.095	14.	95.0-98.5	6	9
1606+106	2 1	.089	4.	94.0-99.0	11	893
1610-771		.271	50.	94.0-99.0	11	202
1611+343	3 1	.088	108.	94.0-99.0	11	899
1614+051	2 1	.186	128.	94.0-99.0	11	68
1622-253	1 1	.208	64.	94.0-99.0	11	931
1622-297		.367	70.	94.0-99.0	10	33
1624+416	3 2	.175	120.	94.0-99.0	8	19
1633+382	3 1	.440	16.	94.0-99.0	10	399
1637+574	2 1	.190	108.	94.0-98.5	9	156
1638+398	1 1	.092	18.	94.0-99.0	11	552
1641+399	4 1	.276	12.	94.5-99.0	7	901
1642+690	3 2	.075	108.	94.0-98.5	8	107
1652+398	3 2	.148	84.	94.5-99.0	10	103
1656+053	3 2	1.510	0.	94.0-98.0	6	33
1657-261		.520	140.	95.0-98.0	5	19
1705+018	2 1	.434	114.	94.0-99.0	11	39
1706-174	2 1	.411	78.	95.5-98.0	5	15
1726+455	2 1	.066	140.	94.0-99.0	11	450
1730-130	2 2	.230	108.	94.5-98.5	7	542
1738+476	2 1	.717	144.	94.0-99.0	5	11
1739+522	2 1	.116	56.	94.0-99.0	11	1135
1741-038	1 1	.134	18.	94.0-99.0	11	1753
1744+557		.191	166.	96.5-99.0	5	9
1745+624	1 2	.069	154.	94.0-99.0	11	252
1749+096	1 1	.094	8.	94.0-99.0	11	1145
1749+701	2 2	.421	76.	94.0-97.0	5	16
1758+388		.176	88.	94.0-99.0	10	17
1803+784	2 1	.071	142.	94.0-99.0	11	1686
1807+698	3 2	.064	154.	94.5-99.0	10	88
1815-553		.959	90.	94.0-98.5	10	96

Table IV-2.4 (cont.)

Source	Struc S X	Sigmax (mas)	Dir (deg)	Data span	Np	Ns
1817-254		.775	90.	94.0-98.5	5	7
1823+568	1 1	.241	104.	94.0-99.0	10	133
1845+797	4 2	.543	38.	95.0-98.5	6	21
1849+670	1 2	.047	44.	94.5-99.0	6	61
1901+319	4 3	.236	26.	94.5-98.5	8	20
1908-201		.123	74.	94.0-99.0	9	126
1920-211		.447	46.	96.0-99.0	6	29
1921-293	2 1	.252	84.	94.0-99.0	11	1084
1928+738	3 2	.277	74.	94.0-98.5	6	97
1936-155	1 1	.344	148.	95.5-99.0	7	21
1937-101	3 1	.387	116.	94.0-98.5	7	11
1954+513	2 1	.361	34.	94.0-98.0	5	18
1954-388		.196	68.	94.5-99.0	10	189
1958-179	1 1	.214	146.	94.0-99.0	11	637
2000-330		1.278	144.	95.5-98.0	5	18
2007+777	3 1	.130	6.	94.0-98.5	9	232
2008-159	1 1	1.198	132.	96.0-98.5	6	31
2037+511	3 3	.056	128.	95.0-99.0	7	208
2052-474		.495	46.	94.0-98.5	9	42
2109-811		.627	152.	94.0-96.5	6	12
2113+293	1 1	.085	92.	94.0-99.0	9	62
2121+053	2 1	.303	38.	94.0-99.0	10	674
2126-158	2 1	1.558	114.	94.0-99.0	10	87
2128-123	3 2	.278	122.	94.0-99.0	11	566
2134+004	4 1	2.040	8.	94.0-99.0	8	708
2136+141	1 1	.113	6.	95.5-99.0	7	113
2145+067	1 1	.125	2.	94.0-99.0	11	1372
2149+056	2 1	.119	138.	96.0-98.5	6	23
2155-152	3 1	.639	114.	95.0-98.0	5	31
2200+420	3 1	.176	104.	94.0-99.0	10	708
2201+315	3 1	.265	120.	94.0-99.0	11	206
2216-038	3 1	.684	86.	94.5-98.5	8	390
2223-052	2 3	.233	76.	94.0-99.0	9	86
2227-088	1 1	.259	52.	94.5-98.5	7	24
2230+114	4 2	.613	16.	94.5-98.5	7	96
2232-488		.574	60.	94.0-98.0	7	11
2234+282	2 1	.213	154.	94.0-99.0	11	1380
2243-123	3 1	.418	84.	94.5-99.0	10	255
2254+074	1 1	.654	92.	95.0-99.0	5	15
2255-282	1 2	.376	68.	94.0-99.0	11	709
2318+049	2 1	.102	156.	95.0-99.0	8	60
2319+272	3 1	.464	78.	94.5-99.0	6	14
2320-035	3 2	.680	68.	95.0-99.0	6	31
2335-027	3 1	.576	94.	96.0-98.5	5	10
2344+092	3 2	.321	50.	94.0-98.0	6	13
2355-106	1 1	.386	70.	94.0-99.0	9	101
2356+385		4.010	90.	94.5-99.0	5	66

OPA time series of source coordinates

A time series of source coordinates was provided by OPA for 52 sources observed in 1999.

Figure IV-2.4 shows the mean difference of coordinates with ICRF-Ext.1 for these sources.

Fig. IV-2.4: Mean coordinate differences with ICRF-Ext.1 over 1999 for 52 sources, derived from OPA time series of right ascensions and declinations.

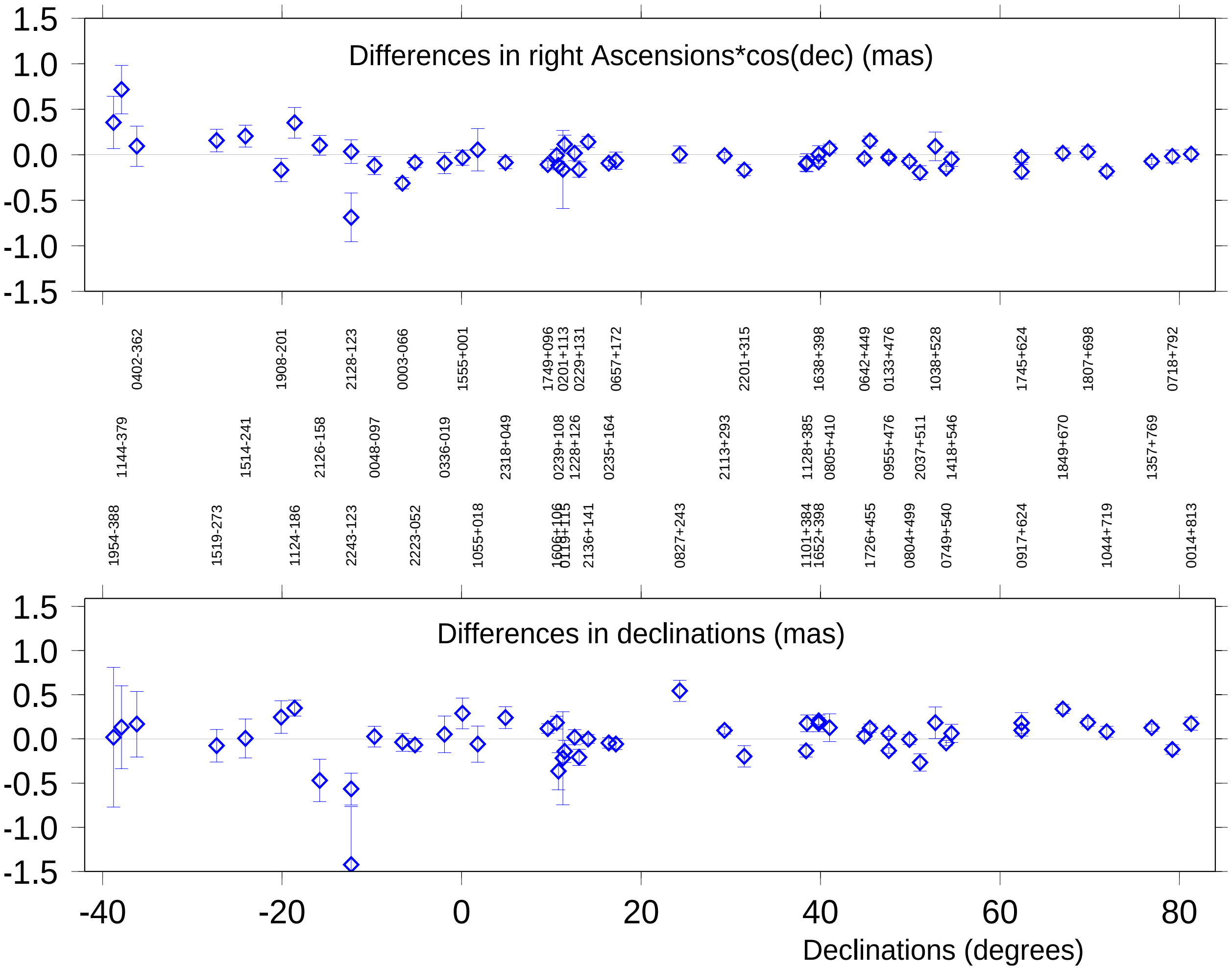

Validation of individual celestial reference frames

The reference frames analyzed

Four extragalactic reference frames obtained from VLBI analysis were submitted to the IERS for inclusion in this report. The analysis strategies used for their calculation are summarized hereafter. The frames have been studied and compared to the ICRF-Ext.1. Notice that some of these catalogues were not optimized for the determination of source positions or for consistency with ICRF or ICRF-Ext.1.

RSC(BKGI) 01 R 01

The celestial reference frame RSC(BKGI) 01 R 01 was elaborated jointly by the Geodetic Institute of the University of Bonn (GIUB) and the Federal Agency for Cartography and Geodesy (BKG). A world-wide set of VLBI observations over the period January 1984 – December 2000 has been analysed with the software *CALC 9.12* and *SOLVE* release *2001.03.07* to obtain from a global solution, radio source positions among other parameters. The celestial frame is aligned to ICRF-Ext.1 by constraining the sum of the right ascension and declination adjustments for the 209 defining sources present in the frame to be zero. Tropospheric gradients have been estimated in the solution.

RSC(GSFC) 01 R 01

Radio source coordinates at the Goddard Space Flight Center have been estimated with *CALC 9.12* and *SOLVE* release *2001.04.20*. The celestial reference frame is attached to the ICRF by a no-net-rotation condition using ICRF defining sources. Positions of the 552 radio sources in RSC(GSFC) 01 R 01 were estimated as global parameters. Quality criteria have been applied for generating the list of sources: either the source has been observed in two or more sessions, in which it had two or more good observations; or the source had at least 25 good observations in the only session it has been observed. 138 sources, which did not fit these criteria, were excluded from the global parameters. Tropospheric gradients have been estimated in the solution for a set of stations.

RSC(IAA) 01 R 02

This celestial reference frame has been obtained with the package ERA v.7 at the Institute of Applied Astronomy of the Russian Academy of Sciences. VLBI sessions of NEOS-A, IRIS-A, IRIS-S, CORE-A and CORE-B networks in the span 1984–2000 were analysed to elaborate a three-step solution.

In a first step, parameters have been adjusted from yearly, one-program solutions. The celestial system is aligned to ICRS by fixing the radio source coordinates to ICRF-Ext.1. At the following step, improved local parameters have been used to perform a similar re-adjustment. RSC(IAA) 01 R 02 results from averaging these yearly, one-program solutions. Tropospheric gradients have been estimated.

RSC(SHA) 01 R 01

MARK III VLBI observations over the period August 1979 – February 2001 were analyzed by the Shanghai Astronomical Observatory. The CALC – SOLVE software was used to produce, from a global solution, the full set of radio source coordinates RSC(SHA) 01 R 01 among other parameters. The celestial reference frame is attached to the ICRF-Ext.1 by applying a no net rotation constraint to the position adjustments of the 212 defining sources with a weighting proportional to the precision of the source positions. Sources with comparatively insufficient observations, so they have large uncertainties, were included in the frame. Tropospheric gradients have been estimated.

Table IV-2.5 gives some characteristics of the four analyzed reference frames. The larger median value for the candidate sources appears in RSC(SHA) 01 R 01.

Table IV-2.5: Analyzed Celestial Reference Frames

Frame	Total	Defining		Candidate		Other		New		Add.	d(°)
	n	n	m	n	m	n	m	n	m	n	
RSC(BKGI) 01 R 01	578	209	0.14	216	0.15	102	0.05	44	0.26	7	-81,+84
RSC(GSFC) 01 R 01	552	202	0.09	201	0.09	101	0.03	35	0.11	13	-81,+84
RSC(IAA) 01 R 02	331	86	0.13	112	0.12	79	0.07	45	0.32	9	-80,+84
RSC(SHA) 01 R 01	675	211	0.15	275	0.23	102	0.04	58	0.28	14	-85,+84

(n) : Number of sources,
(m) : Median of the formal position uncertainty (unit: 0.001"),
(d) : Declination interval (unit: degree).
The column "Add." gives the number of sources in each catalogue not present in ICRF-Ext.1.

Comparison of individual celestial frames with ICRF-Ext.1

Under the assumption that ICRF is free from deformations, we adopt it as a reference to determine systematic effects coming from the current VLBI catalogues.

The comparison algorithm in equations (1) models the global relative orientation between two frames by three angles A_1, A_2, A_3, and the systematic effects by three deformation parameters representing a slope in right ascension as a function of the declination (D_α), a slope in declination as a function of the declination (D_δ), and a bias in declination (B_δ):

$$\begin{aligned} A_1 \,\mathrm{tg}\,\delta \cos\alpha + A_2 \,\mathrm{tg}\,\delta \sin\alpha - A_3 + D_\alpha(\delta - \delta_0) &= \alpha_1 - \alpha_2 \\ -A_1 \sin\alpha + A_2 \cos\alpha + D_\alpha(\delta - \delta_0) + B_\delta &= \delta_1 - \delta_2 \end{aligned} \qquad (1)$$

All individual solutions have been compared to ICRF-Ext.1 by using the model represented in equations (1). Only defining sources common to each frame and ICRF-Ext.1 (or ICRF) were used in the comparisons. The transformation parameters were evaluated by a weighted least squares fit; the equations were weighted using the inverse of the variance of the coordinate differences (α_1–α_2) and (δ_1–δ_2).

Formal uncertainties smaller than 0.01 mas in the individual catalogues have been set to this value. The adjusted parameters serve to transform individual frames into ICRS; the relative global orientation and the deformation parameters are given in Tables IV-2.6 and IV-2.7 respectively.

Table IV-2.6: Relative orientation between individual frames and ICRF

A_1, A_2, A_3 are the rotation angles which transform coordinates from the individual VLBI frames to ICRF. They are calculated on the basis of the defining sources only.
N is the number of common defining sources.
r_α and r_δ are the weighted rms residuals in $\alpha \cos\delta$ and δ respectively.

Frame		N	A_1	A_2	A_3	r_α	r_δ
RSC(BKGI)	01 R 01	209	+0.030 ±0.016	+0.000 ±0.016	-0.050 ±0.021	0.18	0.23
RSC(GSFC)	01 R 01	202	+0.008 ±0.017	+0.001 ±0.017	-0.030 ±0.022	0.18	0.23
RSC(IAA)	01 R 02	86	-0.011 ±0.025	-0.019 ±0.025	-0.032 ±0.039	0.18	0.22
RSC(SHA)	01 R 01	211	+0.032 ±0.015	-0.011 ±0.015	-0.042 ±0.020	0.17	0.22

Unit: 0.001"

Table IV-2.7: Slopes and biases evaluated in the comparisons between individual frames and ICRF

D_α, D_δ are the slopes in right ascension and declination respectively,
B_δ is the bias in declination. They are evaluated in a global solution together with the rotation angles in Table IV-2.5.

Frame		D_α	D_δ	B_δ
RSC(BKGI)	01 R 01	-0.001 ±0.001	+0.000 ±0.000	+0.003 ±0.017
RSC(GSFC)	01 R 01	-0.001 ±0.001	+0.000 ±0.000	+0.043 ±0.018
RSC(IAA)	01 R 02	+0.000 ±0.001	-0.001 ±0.001	+0.013 ±0.032
RSC(SHA)	01 R 01	-0.001 ±0.001	+0.000 ±0.000	-0.011 ±0.016

Units: 0.001"/degree for the slopes, 0.001" for the biases.

In the four submitted frames constraints were applied to align the respective celestial frames to ICRF. The origins of right ascensions in the individual frames agree with the ICRS origin at a few tens of microarcseconds (see values in Table IV-2.6).

The parameters in Table IV-2.7 indicate that there are no slopes in right ascension and declination detected in any individual frames. No strong declination biases are observed; efforts in the modelling in IAA solution and the extension of the frame to lower southern declinations reduced by a factor of ten the bias in declination that was present in previous realizations (catalogues RSC(IAA) 00 R 02 and RSC(IAA) 00 R 03 analysed in the 1999 IERS Annual Report, Table VI-4). The largest bias B_δ (+0.043 mas) appears in RSC(GSFC) 01 R 01. This discrepancy of the GSFC principal plane relative to that of ICRS is removed by the model, as shown when comparing plots IV-2.6 (b) and IV-2.6 (c).

Figures IV-2.5 (a) through IV-2.8 (a) show, for the defining sources common to each analysed frame and ICRF, the postfit residuals in right ascension and in declination as a function of the declination after adjusting the transformation parameters. In all frames compared, the postfit residuals remain at the sub-milliarcsecond level with the exception of a few sources, mainly below the equator.

Figures IV-2.5 (b) through IV-2.8 (b) plot the normalized residuals (ratio of the postfit residual to the uncertainty of the coordinate difference between frames) in declination as a function of right ascension when deformations between frames are not adjusted. Ideally, in absence of deformations, all points should remain within the circle with unit radius shown in the figures.

Figures IV-2.5 (c) through IV-2.8 (c) plot the same parameters when the frames have been freed from the deformations relative to ICRF by the use of the parameters in Table IV-2.7.

In all (b and c) plots the three ICRF categories of sources are shown; filled circles represent the defining sources in each comparison, open circles represent the candidate and other sources.

These plots indicate that the four catalogs are not inconsistent with the ICRF, at its expected level of accuracy (~0,25 mas).

This report was completed by people belonging to the staff of the Paris Observatory component of ICRS-PC, with contributions of three Paris Observatory staff members. They are named below.

Members of the Paris Observatory component of the ICRS-PC:

Souchay[1]	Jean	Co-Director
Arias[2]	Elisa Felicitas	Astronomer
Chapront[1]	Jean	Astronomer
Essaïfi[1]	Najat	Engineer
Feissel[1,3]	Martine	Astronomer
Gontier[1]	Anne-Marie	Astronomer

1. Observatoire de Paris
2. Bureau International des Poids et Mesures
3. Institut Géographique National (France)

Other Paris Observatory staff members :

Carlucci	Teddy	Engineer
Francou	Gérard	Astronomer
Jean-Alexis	Didier	Engineer

For contact information see Section V.3, for electronic access see Appendix.

Fig. IV-2.5: RSC(BKGI) 01 R 01 – ICRF-Ext.1

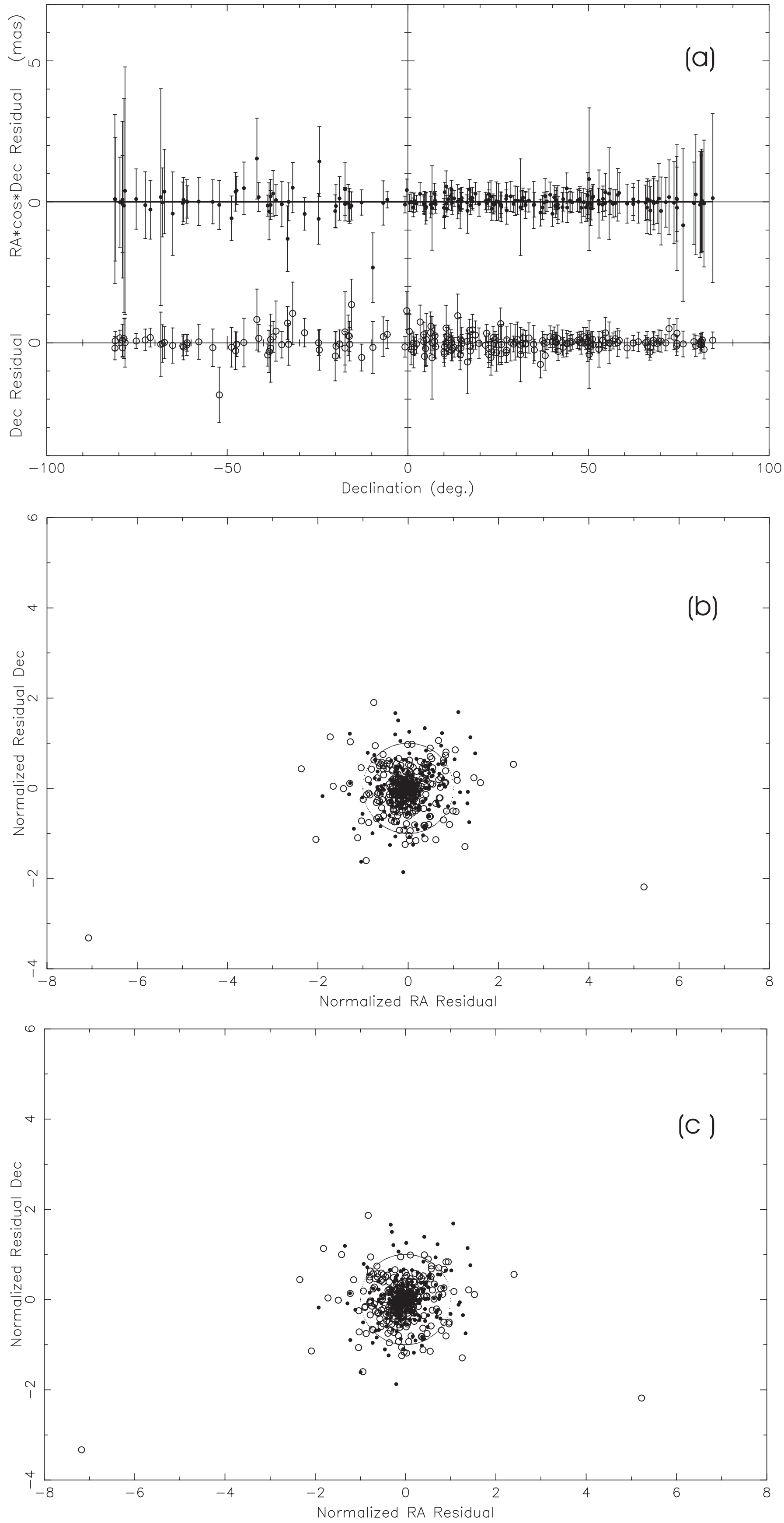

Fig. IV-2.6: RSC(GSFC) 01 R 01 – ICRF-Ext.1

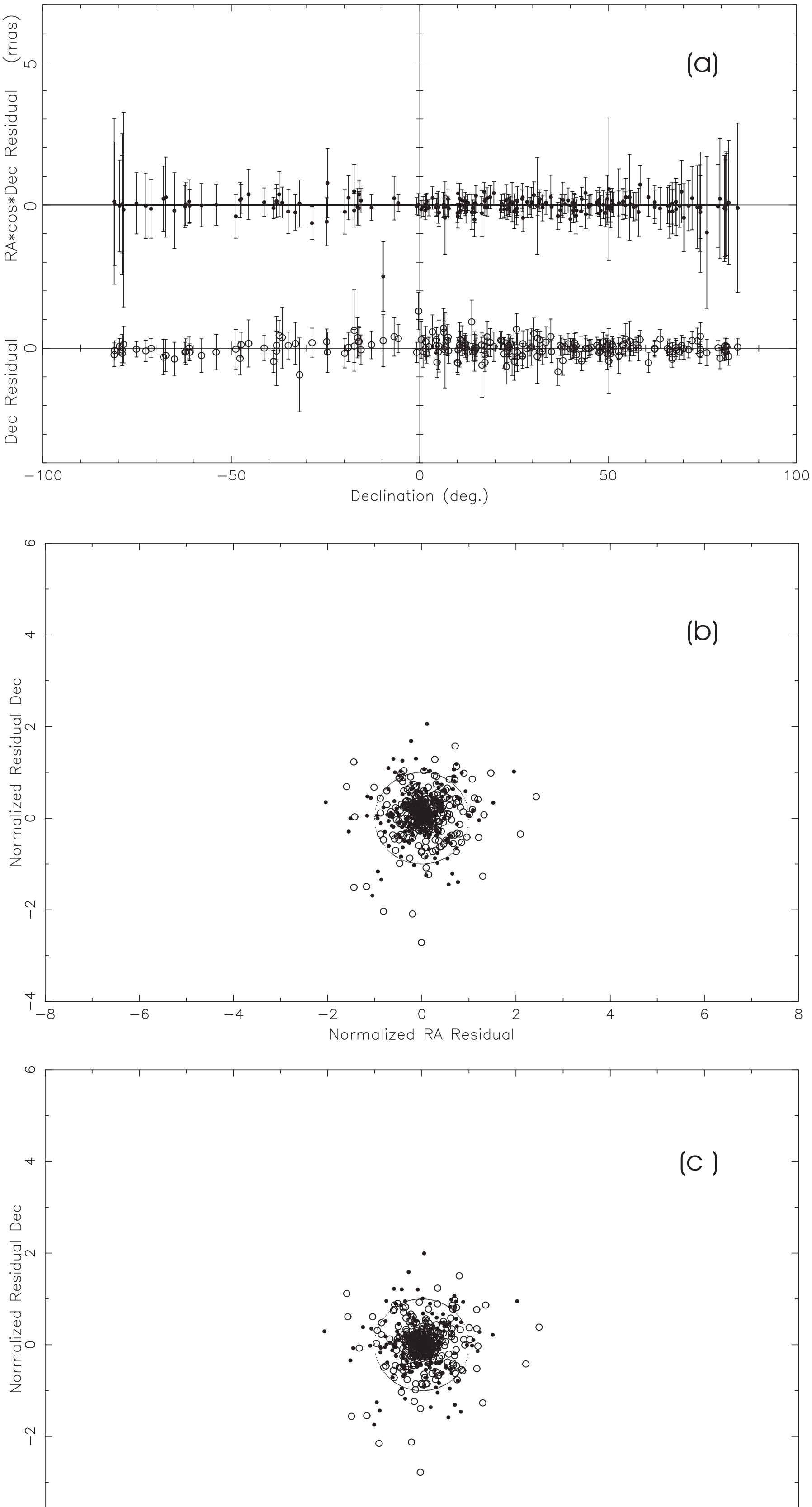

Fig. IV-2.7: RSC(IAA) 01 R 02 – ICRF-Ext.1

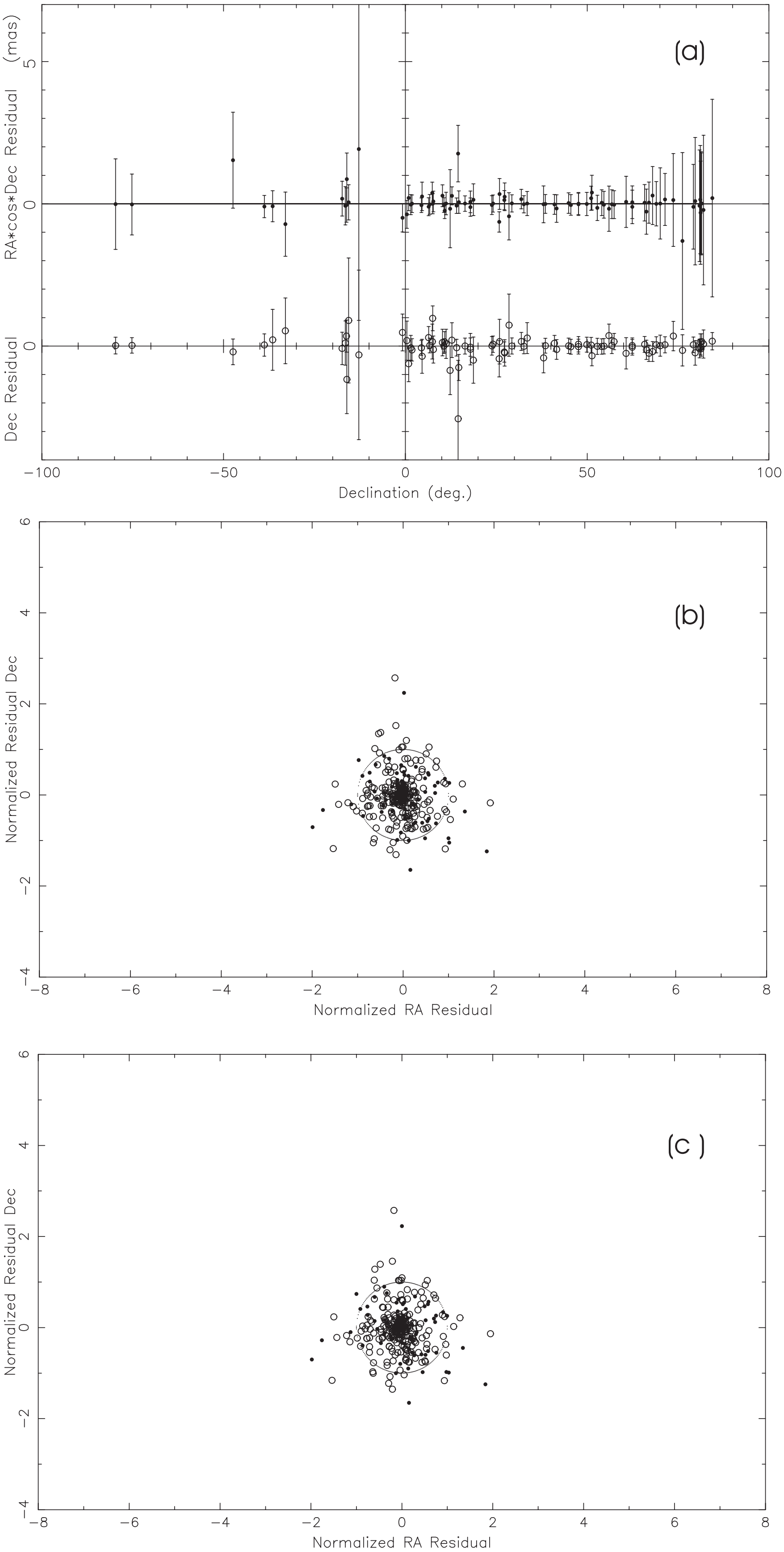

Fig. IV-2.8: RSC(SHA) 01 R 01 – ICRF-Ext.1

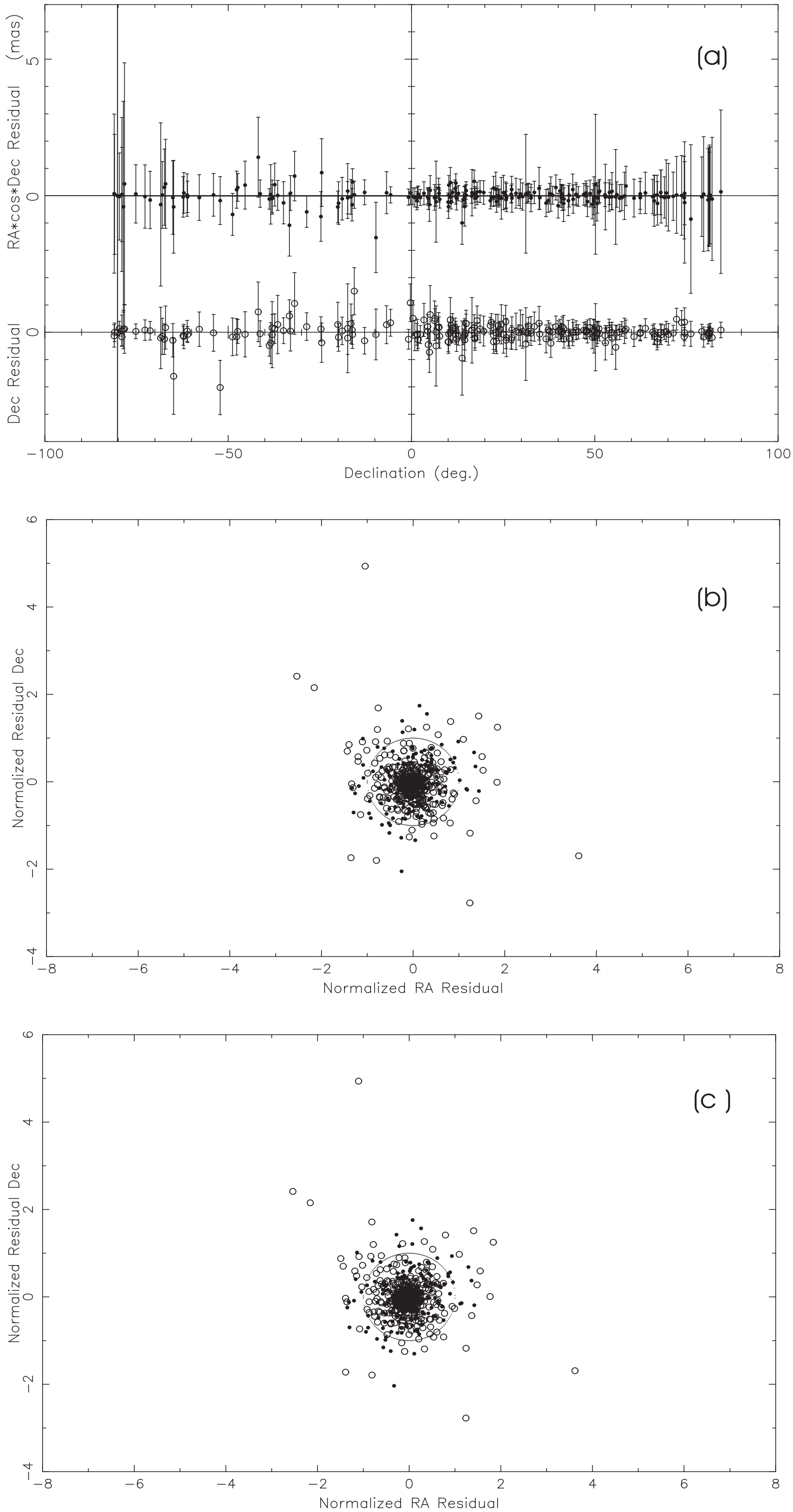

References

Chapront J., Chapront-Touzé M., 1997: Lunar motion, theory and observations, *Celest. Mech.* **66**, 31.

Chapront J., Chapront-Touzé M., Francou G., 1999a: Determination of the lunar orbital and rotational parameters and of the ecliptic reference system orientation from LLR measurements and IERS data, *Astron. Astrophys.* **343**, 624.

Chapront J., Chapront-Touzé M., Francou G., 1999b: Complements to Moons' lunar libration theory. Comparisons and fits to JPL numerical integrations, *Celest. Mech.* **73**, 317.

Chapront J., 2000, Private communication.

Chapront J., Chapront-Touzé M., Francou G., 2001: Contribution of LLR to the reference systems and precession, *in Journées 2000 – systèmes de référence spatio-temporels*, N. Capitaine (ed.), Observatoire de Paris, p. 96.

Feissel M., Mignard F., 1998: The adoption of ICRS on 1 January 1998: meaning and consequences, *Astron. Astrophys*. **331**, L33.

Feissel M., Gontier A.M., Eubanks T.M., 2000: Spatial variability of compact extragalactic radio sources, *Astron. Astrophys*. **359,** 1201.

Folkner W.M., Charlot P., Finger M.H., *et al.*, 1994: Determination of the extragalactic-planetary frame tie from joint analysis of radio interferometric and lunar laser ranging measurements, *Astron. Astrophys.* **287**, 279.

Gontier A.M., Le Bail K., Feissel M., Eubanks T.M., 2001: Stability of the extragalatic VLBI reference frame, *Astron. Astrophys.* **375**, (in press).

Hazard C., Sutton J., Argue A.N., *et al*., 1971: *Nature* **233**, 89.

IERS, 1999: *1998 IERS Annual Report*, Observatoire de Paris, p.87.

Kaplan G.H., Josties F.J., Angerhofer P.E., Johnston K.J., Spencer J.H., 1982 : Precise radio source positions from interferometric observations, *AJ* **87**, 570.

Kinoshita M., Aoki S., 1983: The definition of the ecliptic, *Celest. Mech*. **31**, 329.

Lieske J.M., Lederle T., Fricke W., Morando B., 1977: Expressions for the precession quantities based upon the IAU(1976) system of astronomical constants, *Astron. Astrophys*. **58**, 1.

Ma C., Arias E.F., Eubanks T.M., Fey A.L., Gontier A.-M., Jacobs C.S., Sovers O.J., Archinal B.A., Charlot P., 1997: *IERS Technical Note No. 23*, C. Ma and M. Feissel (eds.), Observatoire de Paris.

Ma C., Arias E.F., Eubanks T.M., Fey A.L., Gontier A.-M., Jacobs C.S., Sovers O.J., Archinal, B.A., Charlot P., 1998: The International Celestial Reference Frame as realized by Very Long Baseline Astrometry, *AJ* **116**, 516.

Mathews P.M., Herring T.A., and Buffett B.A., 2001: Modeling of nutation-precession: new nutation series for non rigid Earth, and insights into the Earth's interior, *J. Geophys. Res.*, (in press).

McCarthy D.D. (ed.), 1992: IERS Standards, *IERS Technical Note No. 13*, Observatoire de Paris.

McCarthy D.D. (ed.), 1996: IERS Conventions, *IERS Technical Note No. 22*, Observatoire de Paris.

Seidelmann P.K., 1982: 1980 IAU Nutation: the final report of the IAU working group on nutation, *Celest. Mech*. **27**, 79.

Simon J.L., Bretagnon P., Chapront J., Chapront-Touze M., Francou G., Laskar J., 1994: Numerical expressions for precession formulae and mean elements for the Moon and the planets, *Astron. Astrophys.* **282**, 663.

Standish E.M., 1981: Two different definitions of the dynamical equinox and the mean obliquity*, Astron. Astrophys*. **101**, L17.

Williams J.G., Melbourne, W.G., 1982: Comments on the effect of adopting new precession and equinox corrections, *in High-precision Earth rotation and Earth-Moon dynamics*, O. Calame (ed.), D. Reidel Publ. Comp., Dordrecht, p. 283.

Williams J.G., 1994: Contributions to the Earth's obliquity rate, precession, and nutation, *AJ* **108**, 711.

Jean Souchay, Elisa Felicitas Arias, Jean Chapront,
Najat Essaïfi, Martine Feissel, Anne-Marie Gontier